

Quantum phase transition of Bose-Einstein condensates on a ring nonlinear lattice

Zheng-Wei Zhou^{1,*}, Shao-Liang Zhang¹, Xiang-Fa Zhou¹, Guang-Can Guo¹, Xingxiang Zhou^{1,†} and Han Pu^{2‡}

¹*Key Laboratory of Quantum Information, University of Science and Technology of China, Hefei, Anhui 230026, P. R. China*

²*Department of Physics and Astronomy, and Rice Quantum Institute, Rice University, Houston, Texas 77251-1892, USA*

We study the phase transitions in a one dimensional Bose-Einstein condensate on a ring whose atomic scattering length is modulated periodically along the ring. By using a modified Bogoliubov method to treat such a nonlinear lattice in the mean field approximation, we find that the phase transitions are of different orders when the modulation period is 2 and greater than 2. We further perform a full quantum mechanical treatment based on the time-evolving block decimation algorithm which confirms the mean field results and reveals interesting quantum behavior of the system. Our studies yield important knowledge of competing mechanisms behind the phase transitions and the quantum nature of this system .

PACS numbers: 03.75.Mn, 67.10.Fj, 05.45.Yv

I. INTRODUCTION

In the past few years, ultracold atoms confined in optical lattices have generated a great amount of excitement in the physics community. They provide the unique opportunity to realize various many-body models that are of fundamental importance in physics [1]. More recently, nonlinear lattices formed by periodically modulating atomic interaction strengths have also received much attention. A comprehensive review of nonlinear wave phenomena supported by nonlinear lattices can be found in Ref. [2]. There are two basic physical systems that can potentially realize nonlinear lattices, both of which can be described by nonlinear Schrödinger equations. One uses electromagnetic waves subject to inhomogeneous nonlinear optical media. The other one is based on atomic Bose-Einstein condensates (BECs) with modulated s -wave scattering length. In this work, we will focus on the latter system although much of the physics are common to both.

We extend our previous work reported in Ref. [3] to study a BEC on a one-dimensional (1D) nonlinear ring-shaped lattice. In Ref. [3], we considered a BEC on this ring lattice whose atomic scattering length is modulated according to

$$a(\theta) = a_0 \sin(d\theta), \quad (1)$$

where θ is the azimuthal angle along the ring and $d = 2$ is the spatial modulation frequency. We have shown that, as the modulation depth a_0 is increased, the condensate can undergo a second-order symmetry-breaking quantum phase transition from a soliton-like state to a spatially periodic condensate that matches the scattering length modulation. In the present work, we generalize our investigation to a larger spatial modulation frequency $d \geq 3$ and compare the results to the $d = 2$ case. We developed a new mean-field technique to study the semi-classical behavior of the system, and found that a similar symmetry-breaking phase transition occurs for $d \geq 3$ as the modulation depth is increased. However, the phase transition is now of *first order*. We also carried out a numerical full quantum mechanical treatment of the system based on the time-evolving block decimation (TEBD) algorithm. Both static and dynamical properties of the system are investigated.

II. THE MODEL HAMILTONIAN

The system considered here is similar to that studied in Ref. [3, 4]. N bosons are confined in a toroid of radius R and cross sectional area S . By sufficiently tightening the radial confinement and freezing the atoms in that direction,

*Electronic address: zwzhou@ustc.edu.cn

†Electronic address: xizhou@ustc.edu.cn

‡Electronic address: hpu@rice.edu

we can treat the atoms as a one dimension system on a ring. The Hamiltonian of the system can be written in the following dimensionless form:

$$H = \int_0^{2\pi} d\theta \left[-\hat{\psi}^\dagger(\theta) \frac{\partial^2}{\partial \theta^2} \hat{\psi}(\theta) + \frac{U}{2} \hat{\psi}^\dagger(\theta) \hat{\psi}^\dagger(\theta) \hat{\psi}(\theta) \hat{\psi}(\theta) \right], \quad (2)$$

where the first term in the integral represents the kinetic energy and the second the interaction energy. For simplicity in notations, we measure energy in units of $\hbar^2/(2mR^2)$. The dimensionless interaction energy $U(\theta) = 8\pi a(\theta)R/S$, where $a(\theta)$ is the periodically modulated s -wave scattering length. In our work, we consider the situation where the scattering length between atoms is modulated along the ring with d periods: $a(\theta) = a_0 \sin(d\theta)$. As in Ref. [4], we define the dimensionless interaction strength as:

$$\gamma(\theta) \equiv -\frac{U(\theta)N}{2\pi} = \gamma_0 \sin(d\theta), \quad (3)$$

where $\gamma_0 = -4a_0RN/S$ represents the modulation depth of the interaction parameter $\gamma(\theta)$.

By taking the Fourier expansion of the field operator $\hat{\psi}(\theta) = \sum_k \frac{1}{\sqrt{2\pi}} e^{ik\theta} \hat{a}_k$, where k takes integer values in order to satisfy the periodic boundary condition and \hat{a}_k is the bosonic annihilation operator for plane wave mode with wavenumber k , the Hamiltonian can be rewritten as:

$$H = \sum_k k^2 \hat{a}_k^\dagger \hat{a}_k + \frac{i\gamma_0}{4N} \sum_{klmn} \hat{a}_k^\dagger \hat{a}_l^\dagger \hat{a}_m \hat{a}_n (\delta_{d+m+n-k-l} - \delta_{-d+m+n-k-l}).$$

Since the number of atoms is fixed, we have $N = \sum_l \hat{a}_l^\dagger \hat{a}_l$. Because of this, the kinetic energy term in the Hamiltonian can also be written as $\frac{1}{N} \sum_{k,l} k^2 \hat{a}_k^\dagger \hat{a}_k \hat{a}_l^\dagger \hat{a}_l$.

III. MEAN-FIELD TREATMENT

In this section, we first consider the mean-field solution valid for $N \gg 1$. In this case, the kinetic energy term can be approximated as

$$\frac{1}{N} \sum_{k,l} k^2 \hat{a}_k^\dagger \hat{a}_k \hat{a}_l^\dagger \hat{a}_l \approx \frac{1}{N} \sum_{k,l} k^2 \hat{a}_k^\dagger \hat{a}_l^\dagger \hat{a}_k \hat{a}_l,$$

and the total Hamiltonian can thus be cast into a biquadratic form as:

$$H = \frac{1}{N} \sum_{i,j,k,l} \alpha_{ijkl} \hat{a}_i^\dagger \hat{a}_j^\dagger \hat{a}_k \hat{a}_l. \quad (4)$$

We will now describe a modified Bogoliubov method we use to find the stationary solution and the excitations of the system.

A. Modified Bogoliubov Approach

In the absence of atomic interactions, the ground state is quite trivial: all the atoms occupy the zero-momentum mode \hat{a}_0 . In the presence of interaction, this is no longer true. However, we may conjecture that the system condenses into a different ground mode $\hat{\chi}_0$. This mode $\hat{\chi}_0$, together with other orthogonal modes $\{\hat{\chi}_i\}$'s that form a complete set, are related to the $\{\hat{a}_i\}$ modes through a unitary transformation U :

$$(\chi_0, \chi_1, \chi_2, \dots)^T = U (a_0, a_1, a_2, \dots)^T. \quad (5)$$

In terms of $\{\hat{\chi}_i\}$ and $\{\hat{\chi}_i^\dagger\}$, the biquadratic Hamiltonian in Eq. (4) takes the following form:

$$\begin{aligned}
H = & \frac{c_0}{N} \hat{\chi}_0^\dagger \hat{\chi}_0^\dagger \hat{\chi}_0 \hat{\chi}_0 + \left(\frac{\hat{\chi}_0^\dagger \hat{\chi}_0^\dagger}{N} \sum_{k,l \neq 0} c_{kl} \hat{\chi}_k \hat{\chi}_l + h.c. \right) + \frac{\hat{\chi}_0^\dagger \hat{\chi}_0}{N} \sum_{k,l \neq 0} d_{kl} \hat{\chi}_k^\dagger \hat{\chi}_l \\
& + \left(\frac{\hat{\chi}_0^\dagger}{N} \sum_{k,l,m \neq 0} p_{klm} \hat{\chi}_k^\dagger \hat{\chi}_l \hat{\chi}_m + h.c. \right) + \frac{1}{N} \sum_{k,l,m,n \neq 0} q_{klmn} \hat{\chi}_k^\dagger \hat{\chi}_l^\dagger \hat{\chi}_m \hat{\chi}_n + \frac{1}{N} \sum_{k,l} r_{kl} \hat{\chi}_k^\dagger \hat{\chi}_l. \quad (6)
\end{aligned}$$

This Hamiltonian can be simplified by a few considerations. First, it is assumed that most atoms will be in the condensate mode $\hat{\chi}_0$. Under the mean field approximation, operators for the macroscopically occupied condensate mode are replaced by c -numbers, i.e., $\hat{\chi}_0, \hat{\chi}_0^\dagger \rightarrow \sqrt{N}$. Since occupation numbers in other $\hat{\chi}_k$ modes are very small, we can drop terms involving 3 or more operators in $\hat{\chi}_k$ and $\hat{\chi}_k^\dagger$ for $k \neq 0$. After this exercise, we obtain the following effective Hamiltonian up to second order in $\{\hat{\chi}_k\}$ and $\{\hat{\chi}_k^\dagger\}$:

$$H_{\text{eff}} = c_0 N + \left(\sum_{k,l \neq 0} c_{kl} \hat{\chi}_k \hat{\chi}_l + h.c. \right) + \sum_{k,l \neq 0} d_{kl} \hat{\chi}_k^\dagger \hat{\chi}_l. \quad (7)$$

This effective Hamiltonian can be diagonalized by the Bogoliubov transformation and the system's elementary excitations are quasiparticles in nature. In order to investigate the stability of the system, we need to analyze the energy spectrum of these quasiparticle excitations. For this purpose, we should work with the following grand canonical operator to account for the conservation of atom numbers:

$$K = H_{\text{eff}} - \mu N. \quad (8)$$

Here, μ is the chemical potential and can be calculated from the condensate energy $E = \langle H \rangle \approx c_0 N$ as:

$$\mu = \frac{\partial E}{\partial N} = c_0 + \frac{\partial c_0}{\partial N} N. \quad (9)$$

Now, we may diagonalize the operator K by using the Bogoliubov transformation on $\{\hat{\chi}_k\}$ and $\{\hat{\chi}_k^\dagger\}$ and obtain the excitation spectrum of quasiparticles. (This will be elaborated on later.) If there is no imaginary excitation frequencies, we claim that the condensate mode $\hat{\chi}_0$ is dynamically stable.

In the above prescription, the key step is to search for the appropriate unitary transformation defined in Eq. (5) that transforms Hamiltonian (4) into (6). Although there are a great number of unknown parameters in the undetermined unitary matrix U , further analysis shows that only the elements in the first row of U are necessary for determining the form of the Hamiltonian (6).

To see this, we note that in order to transform Hamiltonian (4) into (6) via the unitary matrix U , a fundamental requirement is to maintain the biquadratic terms of the operators $(\hat{\chi}_0^\dagger, \hat{\chi}_0)$ and to eliminate all the cubic terms. To this end, we may use the operators $(\hat{\chi}_i^\dagger, \hat{\chi}_j)$ to represent the operators $(\hat{a}_l^\dagger, \hat{a}_m)$ in Hamiltonian (4) via:

$$\hat{a}_i = \sum_j u_{ji}^* \hat{\chi}_j$$

where u_{ij} is the matrix element of the unitary matrix U , and we obtain the following two equations :

$$c_0 = \sum_{i,j,k,l} \alpha_{ijkl} u_{0i} u_{0j} u_{0k}^* u_{0l}^*, \quad (10)$$

$$0 = \sum_{i,j,k,l} (\alpha_{ijkl} + \alpha_{ijlk}) [u_{0i} u_{0j} u_{0k}^* (a_l - u_{0l}^* \chi_0)]. \quad (11)$$

Since $\chi_0 = \sum_i u_{0i} a_i$, Eq. (11) can be recast into a set of equations in operators $\{a_i\}$ (the number of this set of equations depends on the cut-off of the Bose modes) and can be solved by numerical method. Once the representation of the operator χ_0 is determined, the parameter c_0 and the chemical potential μ can be obtained by solving Eqs. (10) and (9), respectively. Therefore, Eqs. (10) and (11) together represent an algebraic form of the Gross-Pitaevskii (GP) equation. In Appendix A, we will show that they are indeed equivalent to the ordinary GP equation. The main

advantage of Eqs. (10) and (11) is that, in principle, all the stationary states (both dynamically stable and unstable ones) of the system can be found. When more than one stable solutions are found, the one that is dynamically stable and with the lowest energy will be identified as the ground state of the system. In contrast, with ordinary GP equation, using imaginary time evolution method one can only find the dynamically stable states, and often just the ground state. Therefore, Eqs. (10) and (11) are superior for studying the phase transitions in our system, where information beyond the ground state is needed.

Once the condensate state is determined, the Bogoliubov spectrum of quasiparticle excitations above it can be found by diagonalizing K defined in Eq. (8) using the Bogoliubov transformation. The details are described in Appendix B.

B. Mean-field quantum phase transition

Using the modified Bogoliubov method outlined in the previous section, in principle we can find all the stationary states (not just the ground state) and their excitation spectrum for any modulated atomic interactions. This provides a more thorough picture of the energy landscape of the system and deeper insights into possible quantum phase transitions induced when certain parameters are varied (in our case, the modulation depth of the interaction strength γ_0).

Our goal is to study the mean field quantum phase transition for different modulation period d as the modulation depth γ_0 is varied. We concentrate on the low-energy states, meaning stationary states with energy close to that of the ground state. We find that there are mainly two types of stationary states in the low energy regime. One type has a density profile matching the modulated period of the scattering length. We refer to such states as symmetric states. The other type features a density profile that spontaneously breaks the symmetry of the modulation. We refer to such states as asymmetric states. The asymmetric states is always d -fold degenerate with the peak density located at $\frac{(1+4i)\pi}{2d}$ ($i = 0, 1, \dots, d-1$), where the local interaction energy $U(\theta)$ reaches the minimum. Under the mean field treatment (MFT), the symmetry-breaking quantum phase transition from the symmetric type to the asymmetric type have been studied for uniform scattering length [4] and for $d = 2$ periodic scattering length [3]. Here, by taking advantage of the modified Bogoliubov method, we investigate the critical point of the quantum phase transitions and the prime mechanism driving such quantum phase transitions for arbitrary modulation period d . We find that there is a fundamental difference between $d = 2$ and $d > 2$.

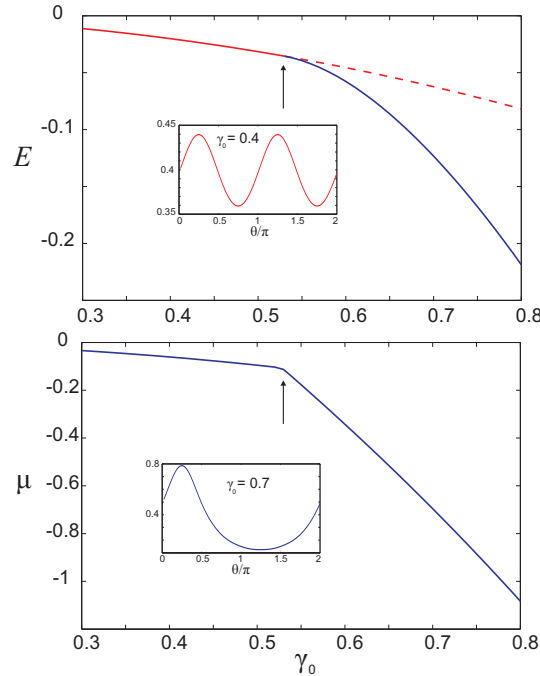


FIG. 1: (Color online) Upper panel: Energy of the condensate for $d = 2$. The red solid line is for the dynamically stable symmetric state, the red dashed line is for the dynamically unstable symmetric state and the blue solid line is for the stable asymmetric state. Lower panel: Chemical potential of the ground state. At the critical point $\gamma_0 = 0.528$ (indicated by arrows in the plots) the ground state changes from the symmetric to the asymmetric type. Shown in the insets are typical wave functions for symmetric and asymmetric states.

Figure 1 shows the energies and chemical potentials of low-energy Bose condensate states by varying the parameter γ_0 for $d = 2$. For small γ_0 , the ground state is a symmetric state. As γ_0 is increased, a symmetry-breaking phase transition occurs at a critical value of $\gamma_0 = 0.528$. At this point, the symmetric state becomes dynamically unstable and the ground state changes to an asymmetric state. The ground state chemical potential shows a kink at this critical point, whereas the ground state energy curve is smooth. This represents a second-order phase transition [3]. A similar behavior is also found in attractive BEC with unmodulated scattering length [4].

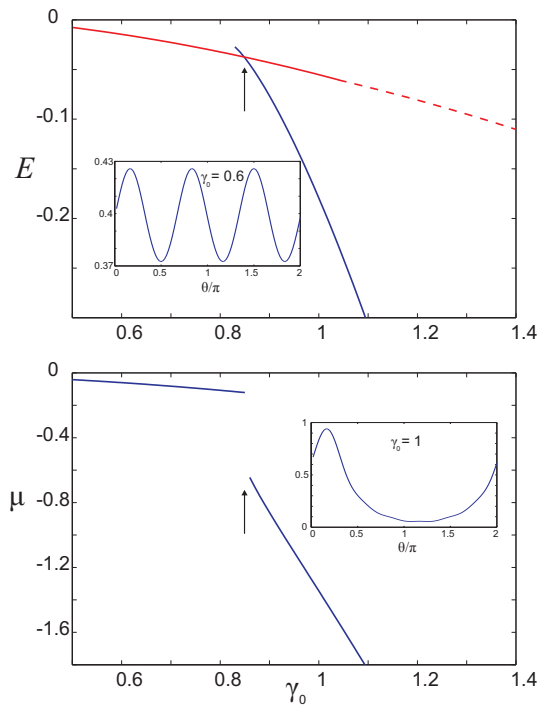


FIG. 2: (Color online) Same plots as in Fig. 1 for $d = 3$. The symmetry breaking phase transition occurs at the critical point $\gamma_0 = 0.85$ (indicated by the arrows in the plots) and the dynamical instability sets in for the symmetric state at $\gamma_0 = 1.04$.

Next, we turn our attention to the case of $d = 3$. The energies and chemical potentials as functions of γ_0 are plotted in Fig. 2. Similar to the $d = 2$ case, for small γ_0 , the ground state is symmetric. As γ_0 is increased, a symmetry-breaking phase transition occurs at a critical value of $\gamma_0 = 0.85$. However, unlike in the $d = 2$ case, at this critical point, the symmetric state remains dynamically stable although the energy of the asymmetric state drops below that of the symmetric state. Furthermore, the ground state energy curve as a function of γ_0 shows a kink at this critical value, while the ground state chemical potential becomes discontinuous at this point. Therefore, the phase transition at this point is of first order. The dynamical instability of the symmetric state does not occur until $\gamma_0 = 1.04$.

To summarize our mean-field results, we have found that the nature of the phase transitions changes for different modulation period d due to the presence of competing mechanisms in this system. When the modulation period $d = 2$, the symmetry-breaking phase transition is of second order and is induced by dynamical instability of the associated states. For $d = 3$, in contrast, the symmetric-breaking phase transition is of first order and is driven by the level crossing of different types of states. We have also investigated the cases for $d = 4$ and 5 and found similar behavior as in $d = 3$.

IV. QUANTUM MECHANICAL TREATMENT

So far, we have limited our discussion to the mean-field approximation. Now we perform a fully quantum mechanical examination of the system using a numerical method. In our previous work [3], exact diagonalization is used for this purpose. Here, we will use the TEBD algorithm [5]. This has a two-fold advantage compared to the exact diagonalization method: (1) It allows us to treat larger systems; and (2) in addition to the static properties, we can also use the TEBD method to study the dynamical behavior of the system.

We first discretize the space by introducing an equidistant grid $\theta_i = i\Delta\theta$, ($i = 0, 1, \dots, M-1$). We then replace the field operator $\hat{\psi}(\theta_i)$ by $\hat{\psi}_i/\sqrt{\Delta\theta}$, where $\hat{\psi}_i$ is a bosonic annihilation operator. In doing so, integrals can be

replaced by sums and the second derivative in the kinetic energy term can be approximated by the difference quotient $\frac{\partial^2}{\partial \theta^2} \hat{\psi}(\theta_i) \approx [\hat{\psi}(\theta_{i+1}) + \hat{\psi}(\theta_{i-1}) - 2\hat{\psi}(\theta_i)] / \Delta\theta^2$. Finally, the discretized Hamiltonian is [6]:

$$H = -\frac{1}{\Delta\theta^2} \sum_{i=0}^{M-1} (\hat{\psi}_i^\dagger \hat{\psi}_{i+1} + h.c.) + \frac{1}{\Delta\theta^2} \sum_{i=0}^{M-1} \hat{\psi}_i^\dagger \hat{\psi}_i + \sum_{i=0}^{M-1} \frac{U_i}{2\Delta\theta} \hat{\psi}_i^\dagger \hat{\psi}_i^\dagger \hat{\psi}_i \hat{\psi}_i. \quad (12)$$

Here, the periodic boundary condition leads to the relation $\hat{\psi}_0 = \hat{\psi}_M$. For TEBD algorithm with periodic boundary condition, we refer to Ref. [7]. In our numerical treatment, we typically divide the ring into $M = 60$ equidistant grids. Our code is adapted from the open source package maintained by the group of Lincoln Carr [8].

A. many-body ground-state energy

In Fig. 3, we plot the ground-state energy per atom of the many-body system as functions of γ_0 for the modulation period $d = 2$ and $d = 3$. We see that the ground-state energy curve approaches the MFT result as N increases, which is consistent with the usual quantum-semiclassical crossover behavior for finite-size quantum systems.

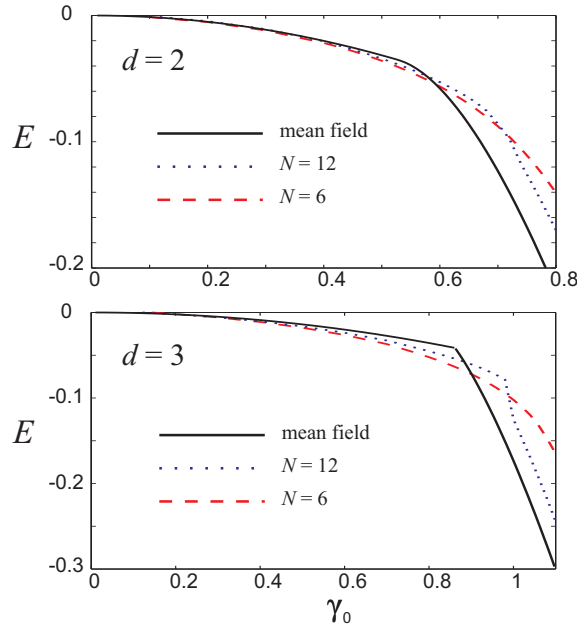


FIG. 3: (Color online) Many-body ground-state energy per atom for $N = 6, 12$ and modulation period $d = 2$ (upper panel) and $d = 3$ (lower panel). The black solid lines are the mean-field results.

B. quantum correlation

In the quantum mechanical treatment, unlike the mean field results, the spontaneous symmetry breaking of density distribution of ground state wavefunction in real space dose not occur. The density profile of the quantum mechanical ground state always matches the spatial modulation of the scattering length [3]. However, we can still gain important insights into the change in the characteristics of the wavefunctions by examining the quantum correlation which is neglected in the mean-field study.

For further discussion, we define the partial number operator between the interval $\theta \in [\varphi_i, \varphi_f]$ as:

$$\hat{n}_{[\varphi_i, \varphi_f]} = \frac{1}{2\pi} \int_{\varphi_i}^{\varphi_f} d\theta \hat{\psi}^\dagger(\theta) \hat{\psi}(\theta). \quad (13)$$

For the particular case of $d = 3$, we define three partial particle number operators as follows:

$$\hat{n}_i = \hat{n}_{[(i-1)\frac{2\pi}{3}, i\frac{2\pi}{3}]}, \quad i = 1, 2, 3. \quad (14)$$

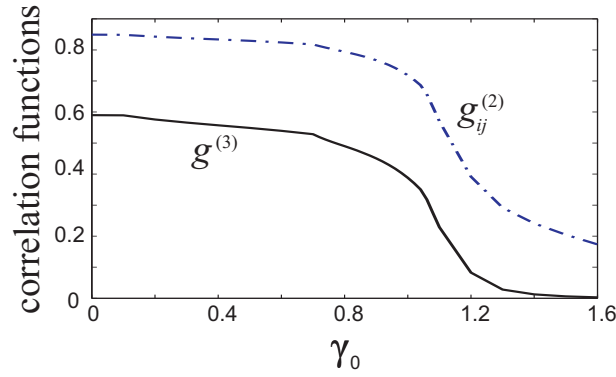


FIG. 4: (Color online) Bipartite correlation $g_{ij}^{(2)}$ and tripartite correlation $g^{(3)}$ as functions of γ_0 for $N = 6$ and $d = 3$.

Using these number operators, we can define the bipartite and tripartite correlation functions as:

$$g_{ij}^{(2)} = \frac{\langle \hat{n}_i \hat{n}_j \rangle}{\langle \hat{n}_i \rangle \langle \hat{n}_j \rangle},$$

$$g^{(3)} = \frac{\langle \hat{n}_1 \hat{n}_2 \hat{n}_3 \rangle}{\langle \hat{n}_1 \rangle \langle \hat{n}_2 \rangle \langle \hat{n}_3 \rangle}.$$

We plot the bipartite and tripartite correlations as functions of γ_0 in Fig. 4. All these correlations are monotonically decreasing functions of γ_0 . In our calculation, the three two-body correlation functions $g_{12}^{(2)}$, $g_{13}^{(2)}$ and $g_{23}^{(2)}$ are essentially identical, which is also expected from the symmetry of the system. At $\gamma_0 = 0$, the ground state is exactly known:

$|\Psi\rangle_{\text{ground}} = \frac{(a_0^\dagger)^N}{\sqrt{N!}} |\text{vac}\rangle$. The theoretical values of bipartite and tripartite correlations can be obtained as:

$$g_{ij}^{(2)}(\gamma_0 = 0) = 1 - \frac{6}{\pi^2 N} \sum_{l=1}^{\infty} \frac{1}{l^2},$$

$$g^{(3)}(\gamma_0 = 0) = 1 - \frac{18}{\pi^2 N} \sum_{l=1}^{\infty} \frac{1}{l^2} + O\left(\frac{1}{N^2}\right),$$

which are in good agreement with the numerical results. When N goes to infinity, all the bipartite and tripartite correlations approach unity at $\gamma_0 = 0$.

Figure 4 shows that although both bipartite and tripartite correlations decay as the interaction parameter γ_0 increases, the tripartite correlation $g^{(3)}$ decays into zero much faster than the bipartite correlation $g_{ij}^{(2)}$. For the case of $N = 6$ as illustrated in Fig. 4, $g^{(3)}$ is essentially zero at $\gamma_0 = 1.6$, while all the $g_{ij}^{(2)}$ are clearly non-zero at the same γ_0 . This is reminiscent of the three-body entangled W -state, which can be written as

$$|W\rangle = \frac{1}{\sqrt{3}} (|100\rangle + |010\rangle + |001\rangle).$$

For the W -state, the tripartite entanglement characterized by the 3-tangle disappears and the bipartite entanglement characterized by concurrence remains finite [9]. For large γ_0 , our mean-field treatment presented earlier reveals that the ground state is characterized by asymmetric state with three-fold degeneracy. Each of these degenerate mean-field state features a density peak at $\theta = (1 + 4i\pi)/6$ ($i = 1, 2, 3$). In the quantum treatment, this degeneracy is lifted by quantum fluctuations, and the non-degenerate quantum ground state may be regarded as roughly a W -state formed by these three mean-field states.

C. Single-particle density matrix

Another important quantity to characterize the many-body state is the single-particle density matrix $\rho^{(1)}$ whose matrix element is defined as [10, 11]:

$$\rho_{ij}^{(1)} = \langle \hat{\psi}_i^\dagger \hat{\psi}_j \rangle, \quad (15)$$

where the expectation value is calculated with respect to the ground state obtained using the TEBD method. Roughly speaking, $\rho_{ij}^{(1)}$ represents the probability amplitude of finding one particle at site i and at the same time another particle at site j .

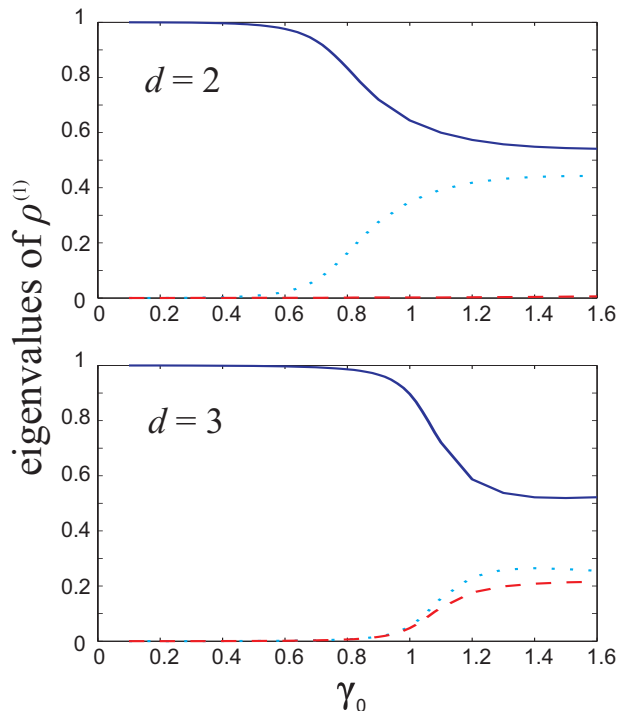


FIG. 5: (Color online) The largest three eigenvalues of the single-particle density matrix $\rho^{(1)}$ for $N = 6$.

Because the matrix $\rho^{(1)}$ is Hermitian it can be diagonalized as:

$$\rho^{(1)} = N \sum_i p_i \varphi_i^* \varphi_i, \quad (16)$$

where the eigenvalues p_i are non-negative and satisfy the constraint $\sum_i p_i = 1$. For a bosonic system with $N \gg 1$, p_i is closely related to the condensate fraction of the system. It is easy to see that, the system will be in a simple condensate state if and only if the largest eigenvalue is of order unity and all the other p_i 's are of order $O(N^{-1})$. If there are multiple p_i 's of order unity, the system is said to be in a fragmented condensate because all the corresponding states have appreciable occupation numbers. Finally, if all the p_i 's are of order $O(N^{-1})$, then the system is not Bose condensed. It is reasonable to speculate that, at small N , the condensate fraction versus the strength parameter γ_0 exhibits quantum crossover behavior. For $N = 6$ with the modulation periods $d = 2$ and $d = 3$, we plot the three largest p_i 's versus γ_0 in Fig. 5. The figure shows that at small γ_0 , the system may be characterized as a simple condensate. It becomes more and more fragmented as γ_0 is increased. In the large γ_0 limit, the eigenvalues approach some steady state values and there are d eigenvalues which are much larger than the rest. This is consistent with the earlier argument that at large γ_0 , the quantum many-body ground state can be roughly regarded as superpositions of the d -fold degenerate mean-field ground states.

To further quantify the crossover from a simple condensate to a fragmented condensate, we adopt two methods as described below. In Fig. 6(a), we plot $dp_0/d\gamma_0$ as a function of γ_0 , where p_0 is the largest single-particle density matrix eigenvalue. In Fig. 6(b), we plot the overlap of the ground-state wave function [12] $|\langle G(\gamma_0) | G(\gamma_0 + \delta\gamma) \rangle|$ for a small value of $\delta\gamma = 0.02$, where $|G(\gamma_0)\rangle$ denotes the ground state at γ_0 . Both of these quantities measure how fast the characteristics of the ground state change as γ_0 is varied. These two measures provide consistent results: both exhibit a dip at some critical value $\gamma_0 = 0.84$ for $d = 2$ and $\gamma_0 = 1.08$ for $d = 3$, which we may define as the critical modulation depth where the system crosses from a simple condensate to a fragmented condensate.

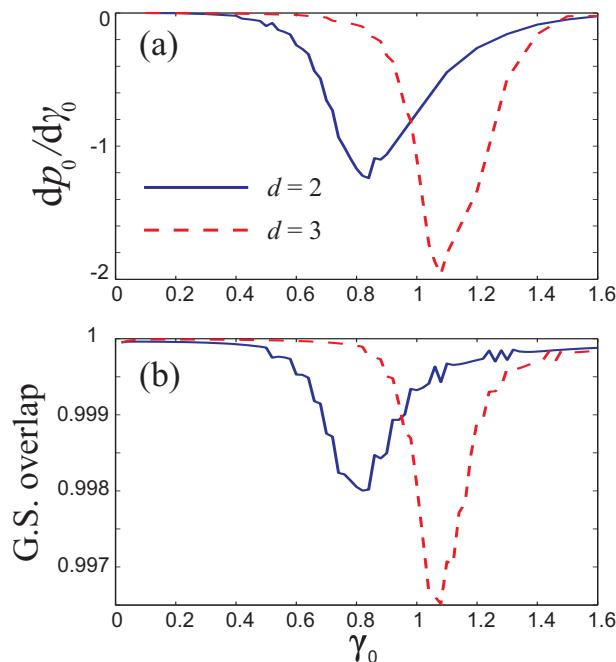


FIG. 6: (Color online) (a) Derivative of the largest single-particle density matrix eigenvalue with respect to the interaction strength modulation depth and (b) overlap of the ground-state wave function versus γ_0 for the particle number $N = 6$.

D. Time evolution of the survival probability

Up to now, we have focused our attention on the static properties of the ground state. The low-energy excitations of the system in the vicinity of the crossover are also important because they expose fine characteristics valuable for understanding the system dynamics in the crossover. A powerful tool to study this is the time evolution of ground state survival probability [13, 14]. It describes the dynamical behavior of the system's ground state under small perturbation in parameters in the system Hamiltonian. In our problem, we parameterize the Hamiltonian using the interaction strength modulation depth γ_0 such that $H = H(\gamma_0)$. If γ_0 has a small variation $\delta\gamma$ so that $\gamma_0 \rightarrow \gamma_0 + \delta\gamma$, the ground state's survival probability is defined as

$$M(t) = |\langle G(\gamma_0) | \exp\{-iH(\gamma_0 + \delta\gamma)t\} | G(\gamma_0) \rangle|^2. \quad (17)$$

The survival probability can be considered as a special case of the quantum Loschmidt echo [15]. Incidentally, the numerical method we used to simulate our system, the TEBD algorithm, is very convenient in calculating the system's time evolution and hence the survival probability.

We calculated the ground state survival probability $M(t)$ and plot the results in Fig. 7 for $N = 6$ and the perturbation in γ_0 is $\delta\gamma = 0.1$. $M(t)$ exhibits roughly sinusoidal oscillations in time. The amplitude of the modulation reaches the maximum near critical points which are consistent with those found in previous static study and shown in Fig. 6. Indeed, the curve for the oscillation amplitude of the ground state's survival probability can be used to predict the overlap between the perturbed and original ground state wave functions which is plotted in Fig. 6(b). The larger the oscillation amplitude in $M(t)$, the more sensitive the ground state wavefunction to the perturbation in the Hamiltonian.

V. SUMMARY

In conclusion, we have made a systematic investigation of a condensate on a nonlinear ring lattice. Our studies show that the properties of the system are sensitive to the modulation period d of the interaction strength. In particular, the meanfield symmetry breaking phase transition is second order when the modulation period d is 2 but first order when $d > 2$, due to competing mechanisms present in the system driving these transitions. Our full quantum mechanical treatment based on the TEBD method reveals the behavior of many important quantities that are essential to the characterization of the system physics.

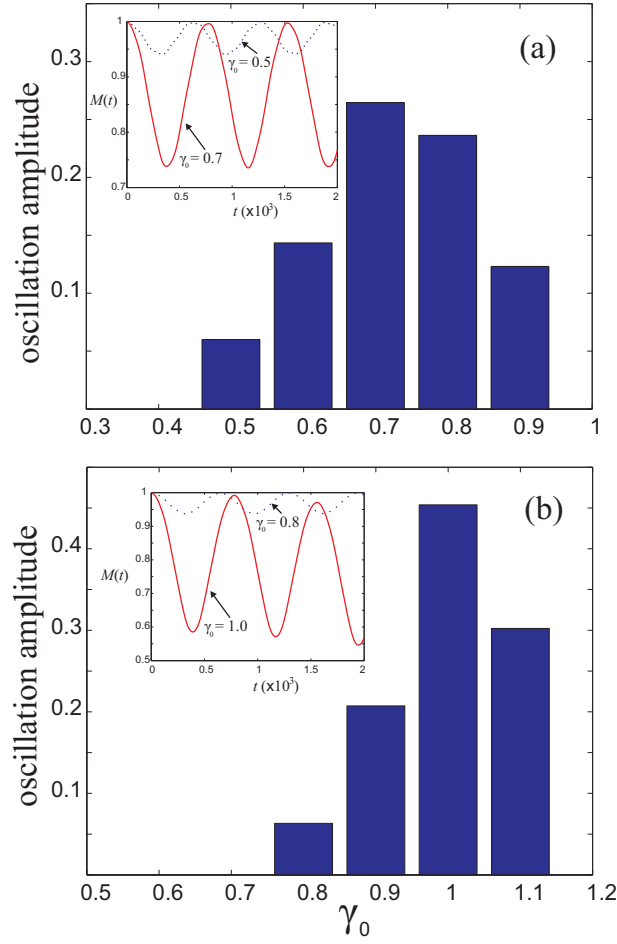


FIG. 7: (Color online) The amplitude of the oscillation of the survival probability $M(t)$ for (a) $d = 2$ and (b) $d = 3$. The inset shows the dynamics of $M(t)$ for different values of γ_0 .

That the mean-field symmetry breaking phase transition changes from second to first order when d changes from 2 to larger than 2 is somewhat surprising. The change of the order of the phase transition may be related to the change of the length scale associated with the modulation of the scattering length: For $d > 2$, this length scale is smaller compared with $d = 2$. Recently, Mayteevarunyoo et al. studied the symmetry breaking transition in a BEC subject to a nonlinear double-well potential and found that the width of the nonlinear potential plays an important role in controlling the transition [16], a phenomenon that may be related to what we discovered in the current work. This is certainly one of the peculiar properties of nonlinear potentials that deserves further investigation.

VI. ACKNOWLEDGMENTS

This work was funded by NFRP 2011CB921204, and NNSF (Grant Nos. 60921091, 10874170, 10875110). Z. -W. Zhou gratefully acknowledges the support of the K. C. Wong Education Foundation, Hong Kong. HP acknowledges support from U.S. NSF. The authors thank Yong-Jian Han, Biao Wu, Shi-Liang Zhu, Hui Zhai, Wu-Ming Liu and Wen-Ge Wang for helpful discussions and comments. Z. -W. Zhou appreciates the hospitality of the Kavli Institute of Theoretical Physics in Beijing, where part of this work was completed.

Appendix A: Proof of the equivalence between the algebraic type and time-independent Gross-Pitaevskii equation

Following the argument in Sec. I, we obtain the Hamiltonian in the limit $N \gg 1$ as

$$H = \sum_{kl} \frac{k^2}{N} a_k^\dagger a_l^\dagger a_k a_l + \frac{i\gamma_0}{4N} \sum_{klmn} a_k^\dagger a_l^\dagger a_m a_n (\delta_{d+m+n-k-l} - \delta_{-d+m+n-k-l}), \quad (\text{A1})$$

which can be written in a simplified form:

$$H = \frac{1}{N} \sum_{ijkl} \alpha_{ijkl} a_i^\dagger a_j^\dagger a_k a_l. \quad (\text{A2})$$

In Sec. III, we obtain the algebraic type GP equations (10) and (11) which we rewrite here as:

$$c_0 = \sum_{ijkl} \alpha_{ijkl} u_{0i} u_{0j} u_{0k}^* u_{0l}^*, \quad (\text{A3})$$

$$0 = \sum_{ijkl} (\alpha_{ijkl} + \alpha_{ijlk}) [u_{0i} u_{0j} u_{0k}^* (a_l - u_{0l}^* \chi_0)]. \quad (\text{A4})$$

Here, there is the unitary relation: $\sum_l u_{0l}^* u_{0l} = 1$. Based on Eqs. (A1) and (A3), we have:

$$c_0 = \sum_{i,j,k,l} \alpha_{ijkl} u_{0i} u_{0j} u_{0k}^* u_{0l}^* = A + B, \quad (\text{A5})$$

where $A = \sum_{kl} k^2 u_{0k} u_{0l} u_{0k}^* u_{0l}^* = \sum_k k^2 u_{0k} u_{0k}^*$ and $B = \frac{i\gamma_0}{4} \sum_{klmn} u_{0k} u_{0l} u_{0m}^* u_{0n}^* (\delta_{d+m+n-k-l} - \delta_{-d+m+n-k-l})$. Furthermore, by considering Eq. (A4), the following relation can be derived:

$$\sum_{kl} k^2 u_{0k} u_{0l} (u_{0k}^* a_l + u_{0l}^* a_k) + \frac{i\gamma_0}{4} \sum_{klmn} u_{0k} u_{0l} (u_{0m}^* a_n + u_{0n}^* a_m) (\delta_{d+m+n-k-l} - \delta_{-d+m+n-k-l}) = 2c_0 \chi_0. \quad (\text{A6})$$

By taking advantage of the unitary relation: $\chi_0 = \sum_l u_{0l} a_l$, Eq. (A6) can be decomposed into the following algebraic equations depending on the boson operator a_l :

$$l^2 u_{0l} + \frac{i\gamma_0}{2} \sum_{kmn} u_{0k} u_{0n} u_{0m}^* (\delta_{d+m+l-k-n} - \delta_{-d+m+l-k-n}) = \mu u_{0l}, \quad (\text{A7})$$

where $\mu = 2c_0 - A = c_0 + \frac{\partial c_0}{\partial N} N$.

The time-independent GP equation describing Bose gases on a ring with periodic scattering length is:

$$-\frac{\partial^2}{\partial \theta^2} \psi(\theta) - 2\pi\gamma_0 \sin(d\theta) |\psi(\theta)|^2 \psi(\theta) = \mu \psi(\theta), \quad (\text{A8})$$

with the boundary condition: $\psi(\theta) = \psi(2\pi + \theta)$. By replacing $\psi(\theta) = \frac{1}{\sqrt{2\pi}} \sum_l u_{0l} e^{-il\theta}$ into Eq. (A8), the algebraic equations same as Eq. (A7) can be derived. This demonstrates the equivalence between Eqs. (10) and (11) and the usual GP equation.

Appendix B: Finding Excitation Spectrum

The Bogoliubov spectrum of quasiparticle excitations can be determined by diagonalizing operator K as defined in Eq. (8). However, here, we can not obtain the representation of Eq. (8) using the modes $\{\chi_l^\dagger, \chi_m\}$ because the unitary transformation U is unknown except for its matrix elements in the first row. This difficulty can be overcome by representing the last two terms at the r.h.s. of Eq. (8) using the original mode operators $\{a_l^\dagger, a_m\}$:

$$K = (c_0 - \mu)N + \sum_{mn} A_{mn} a_m^\dagger a_n + \sum_{mn} (B_{mn} a_m a_n + h.c.), \quad (\text{B1})$$

where $\sum_{mn} B_{mn} a_m a_n = \sum_{i,j,k,l} \alpha_{ijkl} \langle a_i^\dagger a_j^\dagger \rangle : a_k a_l :$ and

$$\sum_{mn} A_{mn} a_m^\dagger a_n = \sum_{i,j,k,l} \alpha_{ijkl} \left\{ \langle a_i^\dagger a_k \rangle : a_j^\dagger a_l : + \langle a_j^\dagger a_l \rangle : a_i^\dagger a_k : + \langle a_i^\dagger a_l \rangle : a_j^\dagger a_k : + \langle a_j^\dagger a_k \rangle : a_i^\dagger a_l : \right\} - \mu \left(\sum_n a_n^\dagger a_n - N \right).$$

Here $\langle A \rangle$ refers to the amplitude of the operator A projecting onto the operators $\chi_0^\dagger \chi_0$, $\chi_0^\dagger \chi_0^\dagger$, or $\chi_0 \chi_0$ and $: A :$ refers to the corresponding component in the operator A orthogonal to the operators $(\chi_0^\dagger \chi_0, \chi_0^\dagger \chi_0^\dagger, \chi_0 \chi_0)$. For instance,

$$\langle a_i^\dagger a_j^\dagger \rangle : a_k a_l := u_{0i} u_{0j} (a_k - u_{0k}^* \chi_0) (a_l - u_{0l}^* \chi_0).$$

To find the energy spectrum for quasiparticle excitation, a generalized Bogoliubov method (see reference [17]) can be used to diagonalize Eq. (B1). Briefly, by introducing the row and column vectors

$$\varsigma = \begin{pmatrix} a \\ a^\dagger \end{pmatrix}, \quad \varsigma^\dagger = (a^\dagger a) \quad (\text{B2})$$

and defining the matrix

$$M = \begin{pmatrix} A & 2B \\ 2B^* & A^* \end{pmatrix} \quad (\text{B3})$$

we may rewrite the operator K as:

$$K = (c_0 - \mu)N + \frac{1}{2} \varsigma^\dagger M \varsigma - \frac{1}{2} \text{Tr} A. \quad (\text{B4})$$

Here, the matrix $A = [A_{mn}]$ and the matrix $B = [B_{mn}]$. Now K can be diagonalized by introducing the appropriate canonical transformation T : $\beta = T \varsigma$. Finally, the operator K has the diagonal form:

$$K = (c_0 - \mu)N + \frac{1}{2} \beta^\dagger \eta T \eta M T^{-1} \beta - \frac{1}{2} \text{Tr} A, \quad (\text{B5})$$

where the matrix $\eta = I \oplus (-I)$ and $T \eta M T^{-1}$ is a diagonal matrix.

-
- [1] I. Bloch, J. Dalibard, and W. Zwerger, Rev. Mod. Phys. 80, 885 (2008).
 - [2] Yaroslav V. Kartashov, Boris A. Malomed, and Lluís Torner, arXiv:1010.2254, to appear in Rev. Mod. Phys.
 - [3] Lisa C. Qian, Michael L. Wall, Shaoliang Zhang, Zhengwei Zhou, and Han Pu, Phys. Rev. A 77, 013611 (2008).
 - [4] R. Kanamoto, H. Saito, and M. Ueda, Phys. Rev. A 67, 013608 (2003).
 - [5] G. Vidal, Phys. Rev. Lett. 91, 147902 (2003); *ibid*, 93, 040502 (2004).
 - [6] B. Schmidt, L. I. Plimak, and M. Fleischhauer, Phys. Rev. A 71, 041601(R) (2005); B. Schmidt, and M. Fleischhauer, Phys. Rev. A 75, 021601(R) (2007).
 - [7] I. Danshita and P. Naidon, Phys. Rev. A 79, 043601 (2009).
 - [8] See <http://physics.mines.edu/downloads/software/tebd/>
 - [9] V. Coffman, J. Kundu, and W. K. Wootters, Phys. Rev. A 61, 052306 (2000).
 - [10] O. Penrose and L. Onsager, Phys. Rev. 104, 576 (1956).
 - [11] A. J. Leggett, Quantum Liquids, Oxford University Press (2006).
 - [12] P. Zanardi and N. Paunković, Phys. Rev. E 74, 031123 (2006).
 - [13] P. Felker and A. Zewail, Adv. Chem. Phys. 70, 265 (1988).
 - [14] W. G. Wang, P. Qin, L. He, and P. Wang, Phys. Rev. E 81, 016214 (2010).
 - [15] A. Peres, Phys. Rev. A 30, 1610 (1984).
 - [16] T. Mayteevarunyoo, B. A. Malomed, and G. Dong, Phys. Rev. A 78, 053601 (2008).
 - [17] J. N. Milstein, The doctoral dissertation: ‘From Cooper Pairs to Molecules: Effective field theories for ultra-cold atomic gases near Feshbach resonances’ (University of Colorado), p118-120 (2004).